Sensors & Actuators: B. Chemical 455 (2026) 139644

Contents lists available at ScienceDirect

Sensors and Actuators: B. Chemical

journal homepage: www.elsevier.com/locate/snb

Thread-based colorimetric biosensor for urea determination in serum

Izabela Lewińska [a,*], Paweł Bącal [b], Ignacio de Orbe-Payá [c,d], Luis Fermín Capitán-Vallvey [c,d], Miguel M. Erenas [c,d,**]

[a] Faculty of Chemistry, University of Warsaw, Pasteura 1, Warsaw 02-093, Poland
[b] Institute of Paleobiology, Polish Academy of Sciences, Twarda 51/55, Warsaw 00-818, Poland
[c] PRIMELab, Electronic and Chemical Sensing Solutions (ECsens), Department of Analytical Chemistry, University of Granada, Granada 18071, Spain
[d] Unit of Excellence in Chemistry Applied to Biomedicine and the Environment of the University of Granada, Granada, Spain

ARTICLE INFO

Keywords:
Urea
Urease
Microfluidic thread-based analytical device
Nanoflowers
Ionophore-based optical sensor

ABSTRACT

Urea is a crucial biomarker in clinical analysis, mainly used to diagnose and monitor kidney condition. However, its reliable determination in serum in point-of-care testing format still remains a vital challenge. Here, we tackled this issue by developing a microfluidic thread-based optical biosensor for serum urea determination. The working principle of the presented device was combining enzymatic urea hydrolysis using urease with the resulting ammonium ions detection using ionophore-chromoionophore chemistry. Urease was immobilized on thread with the aid of synthesized urease-calcium phosphate nanoflowers while components for ammonium ions detection were embedded in PVC-based membrane located on the same thread. In the first step, ammonium ions determination in a thread-based sensor was optimized. Then, urease-calcium posphate nanoflowers (U-CaNFs) were included on the thread to ensure selectivity for urea. U-CaNFs synthesis was optimized and the resulting nanoflowers were characterized using various analytical techniqes (e.g. SEM, EDS, TGA, XRD). The calculated limit of detection for urea was 37 μmol L^{-1} and the total analysis time was only 8 min. The developed thread-based devices were validated with control sera samples, proving their high accuracy.

1. Introduction

Urea is an end-product of protein metabolism, synthesized in the body in the 'urea cycle' or 'the ornithine cycle'. As a final metabolite, urea is excreted from body after its generation, mostly (90 %) in urine formed in the kidneys by glomerular filtration and tubular secretion [1]. Physiological level of urea in blood is between 2.5 and 7.1 mmol L^{-1} while daily urinary urea excretion should be between 12 and 20 g per 24 h. Urea content in blood, often referred to as 'blood urea nitrogen' (BUN), is a valuable clinical biomarker. It is mainly used as a diagnostic parameter for kidneys dysfunction, in which too high BUN is often observed [2]. This is despite its rather low specificity as a kidney conditions biomarker, as BUN level is also influenced by diet, tissue breakdown or gastrointestinal diseases [2]. Urea level in blood is also determined to monitor progression and predict mortality risk in many other diseases e.g. acute and chronic heart failure, community-acquired pneumonia, acute hepatitis A [2].

As a consequence of urea importance in clinical practice, its determination in blood and urine is often requested in clinical laboratories. To meet these demands, various urea determination methods have been described in the literature. These methods can be divided into two categories: direct, relying on direct urea reaction, and indirect. In the second category urea is converted, often enzymatically, to other molecules which are being determined. The most straightforward direct urea determination method is colorimetric Fearon reaction [3]. It relies on reaction of urea with diacetyl monoxime in strongly acidic environment yielding a yellow product, which can be oxidized with ferric chloride to increase sensitivity. However, this method requires heating and suffers from some interferences [3]. Direct electrochemical urea determination protocols usually employ Ni-based material or nanomaterial as a catalyst for urea oxidation reaction. Unfortunately, these methods also suffer from poor selectivity [4]. Indirect methods take advantage of high substrate specificity of urease enzyme to increase their selectivity and they are widely used for urea determination in biological samples. The

* Corresponding author.
** Corresponding author at: PRIMELab, Electronic and Chemical Sensing Solutions (ECsens), Department ofAnalytical Chemistry, University of Granada, Granada 18071, Spain.
E-mail addresses: i.lewinska@uw.edu.pl (I. Lewińska), erenas@ugr.es (M.M. Erenas).

https://doi.org/10.1016/j.snb.2026.139644
Received 29 October 2025; Received in revised form 4 February 2026; Accepted 8 February 2026
Available online 9 February 2026

basic principle of these methods lies in quantification of enzymatic urea hydrolysis products (namely NH_3/NH_4^+ and CO_2/HCO_3) or a change of pH associated with urea hydrolysis. The colorimetric approaches for indirect urea determination utilize Berthelot reaction or its modifications to detect ammonia using alkaline hypochlorite and sodium salicylate [5]. Alternatively, a subsequent enzymatic reaction, catalyzed by glutamate dehydrogenase, can be employed, in which ammonia reacts with 2-oxoglutarate and NADH. The decrease of NADH concentration can be monitored at 340 nm [6]. Electrochemical detection, for example with ammonium ion-selective electrodes or pH electrodes, can also be utilized to determine products of urea hydrolysis [7]. Compilation summarizing the variety and diversity of urea determination methods given in more details can be found in recent review papers [4,5,8,9].

To fulfill a growing demand to perform diagnostic assays outside specialized laboratories, more and more disposable diagnostic tests are presented in the scientific literature and commercialized. These tests are often manufactured on a cheap and biodegradable solid support. Ideally, such support should also promote spontaneous fluid flow by capillary forces to eliminate the need for any external pumping devices. The perfect materials, fulfilling the mentioned requirements, are paper, thread or cloth. While paper and cloth are usually modified with hydrophobic substances or cut to define areas penetrable by aqueous solutions [10,11], thread-based sensing devices take advantage of the default shape of thread and do not require any further modifications [12]. All of the mentioned materials can also serve as a solid support for chemicals immobilization, which react with the target analyte in the introduced sample to produce an analytical response. The resulting analytical devices are inexpensive and user-friendly alternatives to traditional diagnostic analyzers [13].

Several paper- and thread-based analytical devices for urea determination have already been reported in the literature. The vast majority of them rely on urea enzymatic hydrolysis, followed by detection of the pH change using a pH-sensitive dye [14–18]. For this purpose, bromothymol blue have been employed by Ferreira *et al.* in a multilayer paper-based analytical device [14]. The same dye was also utilized in a paper-based device for urea determination proposed by Cheng *et al.* In their work, an optical reader was also described, allowing for blood urea measurement at the point-of-care [15]. Zhang *et al.* to determine urease-mediated pH change utilized Prussian Blue nanoparticles which were immobilized with urease on paper solid support [16]. Phenol red has also been used as an indicator in indirect enzymatic urea determination in a paper-based [17] and thread-based analytical device [18]. On the other hand, detection of products of urea hydrolysis (ammonia and carbon dioxide) has also been utilized to determine urea with the aid of paper-based analytical devices. Sheini developed an origami paper-based analytical device with immobilized urease, thiomalic acid modified silver nanoparticles for NH_3 detection and maltol modified silver nanoparticles for CO_2 detection [19]. Rath *et al.* utilized a change in resistance occurring as a result of a reaction of NH_4^+ ions from urea enzymatic reaction with polystyrene sulfonate [20]. Thread-based analytical devices have also been employed for direct electrochemical urea determination using an electrode modified with NiS and graphene oxide nanocomposite [21]. Finally, thread has also been used to construct analytical systems for electrophoretic separation with electrochemical detection of urea [22,23].

While most of the cited works ensure sufficient analytical performance for urea determination in matrices such as urine, saliva, or milk, reliable determination of this analyte in blood or serum using disposable point-of-care devices remains a significant challenge. Additionally, a true point-of-care analytical device, coherent with ASSURED criteria [24], should avoid using any equipment for signal acquisition. In this paper, we present an updated approach to urea determination relying on its enzymatic hydrolysis and subsequent ammonium ions determination using ionophore-based optical sensor (optode) [25]. Such detection scheme was utilized in the past in macroscopic optical sensors sensitized with urease enzyme [26–29]. Here, inspired by these discoveries, we present a miniaturized device, in which both ammonium-selective optode membrane and urease are immobilized on a single piece of thread. Typically optode membranes are placed on polymeric surface in the form of a thin film [30]. The use of thread as solid support for ion-selective membranes immobilization has been explored by us in the past [31–33]. These works shown that this approach can bring benefits such as short response time, flexibility, and user-friendliness. Moreover, the detection of ammonium ions offers higher sensitivity in comparison to typically employed in urea detection pH sensing. This sensitivity was sufficient to employ unmodified smartphone as an analytical signal reader instead of dedicated equipment [15]. In the first stage of the presented research, the process of ammonium ions determination using ionophore-based optical sensor located on thread was studied and optimized. Then, focus was dedicated to urease enzyme immobilization in the form of urease-calcium phosphate nanoflowers (U-CaNFs) directly on thread support. Finally, the two processes, namely urea hydrolysis to ammonium ions and ammonium ions detection were combined to create a thread-based analytical device for urea determination. The developed sensor was validated with sera samples, demonstrating high accuracy.

2. Materials and methods

2.1. Chemicals and materials

Chromoionophore I, potassium tetrakis(4-chlorophenyl)borate (KClPB), Ammonium Ionophore I (nonactin), poly(vinyl chloride) (PVC), o-nitrophenyl octyl ether (NPOE) and urease from Jack bean (type III, 27520 U g^{-1}) were obtained from Merck (Darmstadt, Germany). Tris(hydroxymethyl)aminomethane (Tris) was purchased from Apollo Scientific (Stockport, UK). Sodium carbonate, tetrahydrofuran (THF), potassium hydrogen phosphate, potassium dihydrogen phosphate, sodium chloride, potassium chloride, magnesium chloride, copper sulfate were from Avantor Performance Materials Poland (Gliwice, Poland). Ammonium chloride, urea and calcium chloride were purchased from Chempur (Piekary Śląskie, Poland). Water used in all experiments (18.2 MΩ cm resistance) was from Milli-RO 12 plus Milli-Q station (Millipore, Bedford, MA, USA). Control human sera with physiological and pathological composition were purchased from Cormay (Warsaw, Poland): Human Normal and Human Pathological, BioMaxima (Lublin, Poland): BioNorm and BioPath and Pointe Scientific (Warsaw, Poland): Pointe N and Pointe P. All sera were reconstituted with purified water according to manufacturers' instructions and diluted with water prior to analysis. Reference urea concentration in these samples was taken from manufacturers' certificate. White cotton thread (caliber 12 and Tex 94) was from Finca (Presencia Hilaturas, Alzira, Spain). To remove wax and hydrophilize thread was washed in boiling 1.0 mol L^{-1} Na_2CO_3 for 1 h, followed by washing with water on ultrasound bath to remove Na_2CO_3 residues. Thread was then dried in room temperature and stored in a closed container until used.

2.2. Ammonium ions detection

Similarly to our previous reports [31–33], 2 cm pieces of washed thread were cut and glued on a piece of double-sided adhesive tape, attached to a piece of paper. Thread was then impregnated with buffer solution by dropping 5 μL of 100 mM Tris pH 7. After buffer has completely dried, 0.5 μL of ammonium-selective cocktail was introduced in the center of thread-based sensor. In the optimal conditions this cocktail consisted of: 1.00 mg Chromoionophore I (23 mmol kg^{-1}), 1.26 mg Ammonium Ionophore I (23 mmol kg^{-1}), 0.85 mg KClPB (23 mmol kg^{-1}), 23.0 mg PVC and 45.0 mg NPOE dissolved in 1 mL of THF. Cocktail was diluted 3-fold in THF prior to deposition on thread. Finally, 10 μL of standard/sample was introduced at one end of μTAD, which was then guided through the entire device owing to capillary forces. After 1 min, the color of the membrane was captured as described in Section 2.5. A scheme of μTAD preparation and NH_4^+ ions detection is

shown in Fig. 1A, while photos of μTAD subjected to low and high NH_4^+ concentration are presented in Fig. S1.

2.3. Urease hybrid nanoflowers synthesis and characterization

Organic-inorganic hybrid nanoflowers were employed to immobilize urease enzyme. The inorganic component of these nanoflowers was calcium phosphate while organic moiety constituted of urease. Initially, urease-calcium phosphate nanoflowers were synthesized by mixing 125 μL 200 mmol L^{-1} $CaCl_2$, 500 μL 200 mmol L^{-1} PBS pH 6.7 with 5 mg mL^{-1} urease and 4.375 mL water, similarly to other reports of urease-calcium phosphate nanoflowers [34,35]. This mixture was incubated for 16 h in 20°C to allow nanoflowers to assembly. Then precipitate was transferred to a centrifuge tube and centrifuged for 15 min at 6000 rpm using IKA mini G centrifuge (Staufen, Germany). The resulting supernatant was discarded, U-CaNF precipitate was resuspended in 1.5 mL of water and centrifuged again. This washing procedure was repeated three times. Finally, U-CaNFs precipitate was suspended in 1 mL 100 mmol L^{-1} Tris pH 7 to be introduced on thread. In the optimized conditions, urease concentration in PBS was switched to 2.5 mg mL^{-1} urease and U-CaNF precipitate was suspended in 0.5 mL of 100 mM Tris buffer pH 7.

U-CaNF were characterized using various experimental techniques. The thermogravimetric analysis (TGA) was done using Mettler-Toledo TGA/DSC STAR^e apparatus. The sample was weighted using Mettler-Toledo XS105 DualRange balance. The powder diffraction (pXRD) measurements were performed using Bruker D8 Advance apparatus with CuKα1 (λ = 1.54 Å) source of radiation and with PSD Vantec detector and the Bruker DIFFRAC PLUS software. A low-background sample holder was employed. Both the TGA/DSC analysis and XRD measurements were done in the Laboratory for Structural and Biochemical Research (LBSBio), Biological and Chemical Research Centre, University of Warsaw. Warsaw, Poland.

The NFs morphology in microscale and elemental composition were analyzed by Scanning Electron Microscope (SEM) with Energy Dispersive X-ray Spectrometry (EDS). The microscope used was a Thermo Fisher Quattro S SEM in the Laboratory of Scanning Electron Microscopy, Institute of Paleobiology, Polish Academy of Sciences, Warsaw, Poland. This is an environmental SEM, which allows for imaging and analysis in higher than typical pressure in microscope chamber. Here, to maintain elevated pressure, and among others to reduce effect of charging of the samples, a H_2O vapor was used. This allows for imaging of non-conductive samples, semi-hydrated samples or fragile samples which poorly withstand sputtering. The SEM was equipped with an Octane Elect (EDAX) EDS detector. The accelerating voltage during imaging was kept in the 5–20 kV range and during elemental composition measurements at 10 or 20 kV. Imaging of non-sputtered samples was done in low vacuum mode (50 Pa) or in high vacuum mode with use

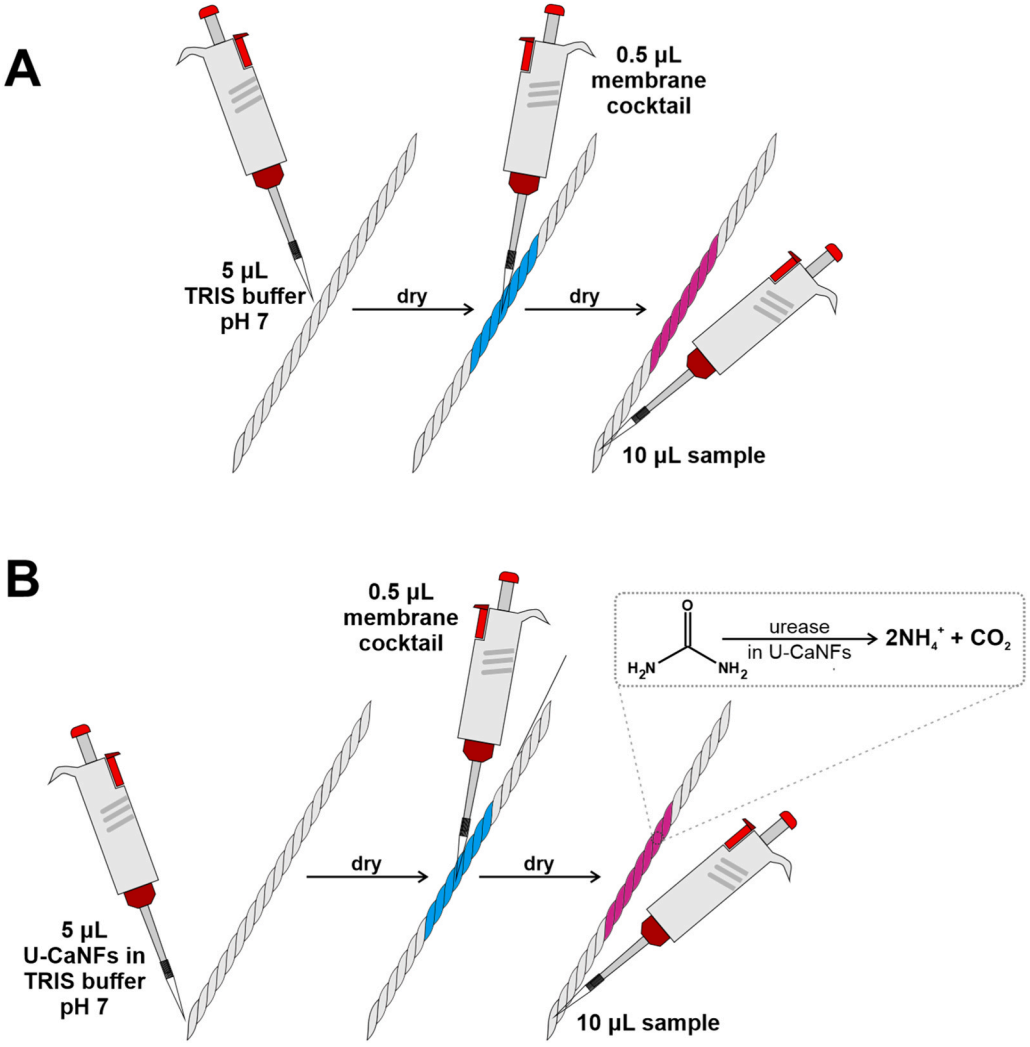

Fig. 1. A: Scheme of μTAD for ammonium ions determination preparation and ammonium ions detection. B: Scheme of μTAD for urea determination preparation and urea detection. U-CaNFs – urease – calcium phosphate nanoflowers.

of ultralow beam currents. Imaging was done employing: secondary (SE) and angular backscatter electron (BSE) detectors. To increase plasticity and to better understand complexity and shape of NFs, some images were obtained as superimposition images from the two detectors mentioned above. For EDS measurements, to minimize the number of charging artifacts, mapping and elemental analysis was done on Pt-sputtered samples or carbon coated samples. The samples were coated with a carbon layer using CCU-10 Safematic sputter or thin coated with Pt using Balt-Tec SCD 005 sputter. Samples were prepared by drying small amounts of NFs solution on standard SEM stub decorated with dedicated substrate material. 5 μL of NFs solutions with differing concentrations were left to dry under ambient conditions. This allows for both smearing and creation of 'coffee rings'. Various substrate materials for sample preparation were tested including Al-foil, Cu-foil, conductive carbon adhesive tape or clean standard SEM-stub (aluminum). EDS mapping of elemental composition/distribution among larger samples (e.g. pieces of thread) was done using Montage Large Area Mapping, a add-in feature of APEX software allowing precise large-area imaging and EDS.

2.4. Urea detection

The working principle of a μTAD for urea determination relies on urea enzymatic hydrolysis to ammonium ions, catalyzed by immobilized on thread U-CaNF, followed by colorimetric ammonium ions detection by ammonium ions-sensitive optode film located in the same thread. A scheme of the occurring reaction is shown in Fig. 1B. The μTADs were prepared similarly to these for NH_4^+ ions detection (Section 2.2). Instead of thread impregnation with Tris buffer, 5 μL of U-CaNF suspension in Tris buffer was introduced in the beginning of the thread. Owing to capillary forces, this solution spread through the thread, allowing for proper buffering of the samples and leaving U-CaNF immobilized in the initial part of the thread-based device. After drying in the ambient conditions, 0.5 μL of ammonium ions-sensitive cocktail was introduced in the middle of the thread. μTADs were stored in the darkness until 10 μL of sample/standard was added at the same end of the thread where U-CaNF suspension was previously introduced (see Fig. 1B). Photos of μTADs subjected to low and high urea concentration are shown in Fig. S1.

2.5. Colorimetric signal acquisition and processing

As a consequence of NH_4^+ ions extraction to the membrane phase and chromoionophore deprotonation, a color change from blue to pink occurred. To quantitatively measure this change of color, μTADs were photographed using Samsung Galaxy M31s smartphone (Suwon, South Korea). The application employed for this purpose was Footej Camera 2 set to ISO 400, shutter speed 1/250 s and auto white balance. To ensure constant lighting, μTADs were placed in an illumination box purchased from Puluz (China) equipped in two LED strips (20 LEDs each, 1100 lumen in total, 5500 K color temperature). The obtained photographs were then transferred to a PC and analyzed with ImageJ software (National Institutes of Health, USA). Firstly, a region of interest (ROI) was selected using brush tool to cover the entire colored region. Then, photos were converted from RGB to HSV color spacer using Color Space Converter functionality of ImageJ. Finally, mean hue (H) was measured inside ROI, which is the recommended analytical signal for bitonal colorimetric sensors [36]. To register reaction kinetics, a video was shot and cut to frames with Avidemux software, which were then analyzed in the same way as photographs. Unless stated otherwise, each measurement was conducted in triplicate, using a new μTAD each time, and the obtained H intensities were averaged.

3. Results and discussion

3.1. Optimization of ammonium ions detection

The detection mechanism of NH_4^+ ions relied on chromoionophore-ionophore chemistry, in which analyte cation is extracted to the hydrophobic membrane phase leading to deprotonation of chromoionophore (lipophilic pH indicator) and a change of its color. NH_4^+ detection process can be summarized in the following equation:

$$\overline{L} + \quad \overline{HI^+} + \quad \overline{R^-} + \quad NH_4^+ \leftrightarrow \quad \overline{LNH_4^+} + \quad \overline{I} + \quad \overline{R^-} + \quad H^+ \qquad (1)$$

where L is Ammonium ionophore I, I is Chromoionophore I and R^- is tetrakis(4-chlorophenyl)borate. A line above symbols indicates lipophilic membrane phase. For more details on cations detection using chromoionophore-ionophore chemistry refer to [31,33].

In the first stage of the project, thread-based optical detection of NH_4^+ ions was optimized to provide sensitive sensor response with low detection limit. All membrane components (23 mg PVC, 45 mg NPOE, 1.2 mg Ammonium ionophore I, 1.0 mg Chromoionophore I and 0.8 mg KClPB) were dissolved in 1 mL THF. To optimize cocktail dilution, this solution was diluted 2, 3, and 4-fold in THF and introduced on thread buffered with Tris buffer pH 7 as described in Section 2.2. In these three conditions a calibration curve in the range from 10^{-6} to 10^{-1} mol L^{-1} NH_4^+ was registered. The obtained results, presented in Fig. S2A, indicate that the widest measuring range is achieved for 3-fold cocktail dilution. Then, two Tris buffers of different pH values (7 and 8) were tested. The concentration of each buffer was 100 mmol L^{-1}. Again, a calibration curve for NH_4^+ were measured in both conditions. As shown in Fig. S2B, the widest measuring range is obtained in pH 7, although pH 8 buffer ensures higher sensitivity in low NH_4^+ ions concentration range. Taking under consideration the expected level of urea in serum (in the millimolar range), we decided to use pH 7 Tris buffer in further studies. Finally, the composition of the membrane was optimized. Chromoionophore concentration was fixed at 23 mmol kg^{-1} and the molar ratio of chromoionophore to salt to ionopore (I:R^-:L) was altered. To establish the optimal KClPB content, cocktails with 1:1:1, 1:1.25:1 and 1:1.5:1 I:R^-:L molar ratios were tested. The obtained data (Fig. S2C) point to 1:1:1 molar ratio as the optimal one. To finalize the optimization process, the influence of ionophore concentration on the calibration dependencies was investigated. The following I:R^-:L ratios were tested: 1:1:0.75, 1:1:1, 1:1:1.5 and 1:1:2. 1:1:1 ratio provides the widest measuring range (Fig. S2D) so it was chosen for further experiments. To conclude this section, the optimal cocktail for NH_4^+ ions detection consists of PVC, NPOE, and chromoionophore, ionohphore and KClPB in 1:1:1 molar ratio (23 mmol kg^{-1} each). Thread should be buffered with 100 mM pH 7 Tris buffer. The cocktail should be diluted 3-fold prior to deposition on thread.

In the optimal conditions, a calibration curve for NH_4^+ ions was registered and it is presented in Fig. 2. Each standard was analyzed in five replicates. The obtained data were fitted with Boltzmann sigmoidal function, which is typically used for optode-based sensors. Limit of detection was calculated as NH_4^+ concentration corresponding to blank signal with 3.3 standard deviations and it was found to be 8.7 μmol L^{-1}. The developed μTAD is characterized by high precision of the readings: 0.73 % for 10 mmol L^{-1} NH_4^+ and 0.66 % for 0.1 mmol L^{-1} NH_4^+. The selectivity of μTAD towards ammonium ions was investigated using separate solutions method (SSM) [37]. Response curves were measured in a chloride salt of each tested interferent. The distance between response curves for main and interfering cations were measured at 0.5 ° of chromoionophore protonation. The tested potentially interfering ions were: Na^+, K^+, Ca^{2+} and Mg^{2+}. The calculated selectivity coefficients ($\log K^{opt}_{NH_4^+-X^{n+}}$) were −2.91 for Na^+, −1.56 for K^+, −2.01 for Ca^{2+} and −2.48 for Mg^{2+}. A respective figure is presented in ESI as Fig. S3. As expected [38], the major interferent in NH_4^+ detection is K^+ ion due to their size and charge similarity. Based on the obtained data, it can be

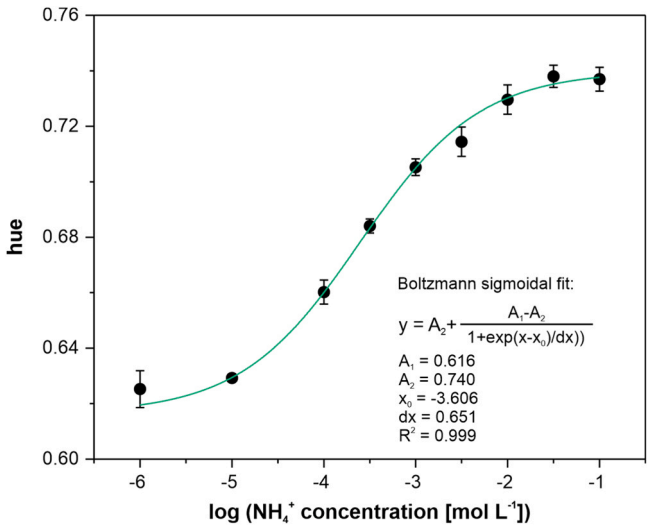

Fig. 2. Calibration curve for ammonium ions registered using the developed μTAD, n = 5.

anticipated that the presence of K^+ ions in serum might affect accurate NH_4^+ determination. However, since the purpose of NH_4^+ ions detection is enzymatic urea determination, the background signal should be subtracted to account for any intrinsic ammonium ions (i.e. these not resulting from urea hydrolysis). In this step, the influence of other interfering ions would be minimized as well. The influence of other potentially interfering compounds was not examined, because any interferences not resulting from alkaline and alkaline-earth cations are unlikely to occur. This is because of membrane permselectivity and hydrophobicity [39].

3.2. Urease-calcium phosphate nanoflowers

Successful enzyme immobilization is often a crucial step in biosensors development. In this project, urease enzyme, which catalyzes urea hydrolysis to NH_3 and CO_2, was immobilized on thread in the form of urease-metal phosphate hybrid nanoflowers. This method of enzyme immobilization has been gaining significant attention in the recent years due to its simplicity and beneficial influence on enzyme stability and activity [40]. Encouraged by the literature [41], we initially attempted to synthesize urease-copper phosphate hybrid nanoflowers to immobilize urease enzyme. The synthesis was conducted according to the recipe given in the literature [41]. The resulting nanoflowers had a well-defined flower-like structure as shown in SEM picture in Fig. S4. However, no enzymatic activity was detected when these nanoflowers were immobilized on thread with NH_4^+-selective membrane. The measured signals for 0, 1 and 10 mmol L^{-1} urea (Fig. S4) did not differ, which indicates that enzymatic hydrolysis of urea did not occur. Possibly, Cu^{2+} ions inhibited urease during nanoflowers synthesis [42], yielding non enzymatically active hybrid nanoflowers. To resolve this issue, copper ions were replaced by calcium ions, which do not have urease enzyme inhibiting properties. U-CaNFs were synthesized and introduced on thread according to Section 2.3 and Fig. 1. In such experimental setup, the signals for 0, 1 and 10 mmol L^{-1} urea could be clearly distinguished (Fig. S4), indicating that urease within U-CaNF retains its enzymatic activity to cause urea hydrolysis.

The synthesis of U-CaNF was optimized to find a combination of parameters which ensures both a well-established flower structure of nanoflowers and sufficient enzymatic activity to enable reliable urea detection in a reasonable time. In each optimization experiment, U-CaNF were prepared in different conditions by changing the concentration of one substrate at a time. The parameters selected for optimization were: calcium ions concentration, phosphate buffer concentration and urease concentration. Incubation time and temperature were fixed at 16 h and 20°C, respectively. To evaluate enzymatic activity of the immobilized urease, a procedure described in Section 2.4 was followed. Signal intensities for 0, 1 and 10 mmol L^{-1} urea were measured using each of the synthesized U-CaNF immobilized on a μTAD. Photographs of μTADs were captured after 10 min after sample introduction. The results of these experiments are shown in Fig. S5. The largest signal difference between the studied urea standards were obtained for nanoflowers prepared with 5 mmol L^{-1} Ca(II) ions and 20 mmol L^{-1} PBS. Both of these conditions were the central values of the tested concentration range, indicating that there is an optimum for Ca (II) ions and phosphate ions concentration for U-CaNFs synthesis. When it comes to urease concentration, the largest it was, the larger difference in signal was measured. 0.25 mg mL^{-1} urease was selected as the optimal enzyme concentration instead of the highest of tested urease concentrations – 0.5 mg mL^{-1}. This is because SEM analysis (Fig. S6) revealed that increasing urease concentration leads to a loss in petal-like nanostructure of the nanoflowers which might affect their properties, as high surface to volume ratio is one of key features of enzyme-metal phosphate nanoflowers.

U-CaNFs synthesized in the optimal conditions were characterized using SEM, EDS, thermogravimetry and powder XRD. A representative selection of SEM pictures registered either without or with conductive carbon sputtering are shown in Figs. 3A and 3B, respectively. The nano petal-like structure of the obtained nanoflowers is better visible without sputtering. However, pictures of non-sputtered, poorly conductive structures have lower resolution than sputtered ones, yet non-sputtered seems to preserve better 3D arrangement of those fragile and delicate structures. This is due fact that these samples are subject of less procedures before imaging and visualized in less harsh conditions (higher humidity and pressure). Because of this, SEM pictures registered in both conditions are presented here. The obtained U-CaNFs have a wide size distribution, ranging from around 4 to over 10 micrometers. Their aspect ratio also varies in the sample, but they rarely are round unlike U-CuNFs shown in Fig. S5B. EDS mapping of U-CaNF was also conducted and the obtained maps are shown in Fig. S7. The EDS were performed with several electron high tensions in range 5–20 kV. As could be expected, such minute and openwork structures reveal only weak signals for light elements. However, peaks for all can be distinguished from background spectra. No signal of C, N, P can be detected in surroundings of U-CaNFs structures. These data clearly prove, that U-CaNFs are composed of oxygen, calcium, phosphorus, carbon and nitrogen, and that the distribution of these elements in the nanoflower is uniform. Thermogravimetric analysis of U-CaNFs was also performed. An initial (up to 180ºC) loss in sample weight is associated with the loss of hydration water (6.77 % of total mass). The second step in weight loss (4.84 % of total mass), occurring between 180 and 540ºC, is caused by organic macromolecule decomposition. As shown in [34], such a result indicates that the vast majority of U-CaNFs mass constitutes of calcium phosphate and only a small fraction is urease. Finally, powder X-Ray diffraction patterns were registered for U-CaNFs. The obtained patterns are consistent with patterns for $Ca_3(PO_4)_2{\cdot}2\,H_2O$, which proves that the crystal component of U-CaNFs is calcium phosphate. For more detailed instrumental characterization of urease-calcium phosphate hybrid nanoflowers, including X-ray photoelectron spectroscopy, nitrogen absorption-desorption study and infrared spectroscopy, please consult a recent paper by Wan *et al.* [34].

3.3. Urea determination optimization

The goal of the next stage of the project was to combine enzymatic hydrolysis of urea and colorimetric detection of the resulting ammonium ions. Urea hydrolysis is catalyzed by urease, immobilized in calcium phosphate nanoflowers, synthesized in the optimal conditions established in Section 3.2. All experiments aimed at obtaining the most sensitive response to urea, while maintaining high precision of the readings

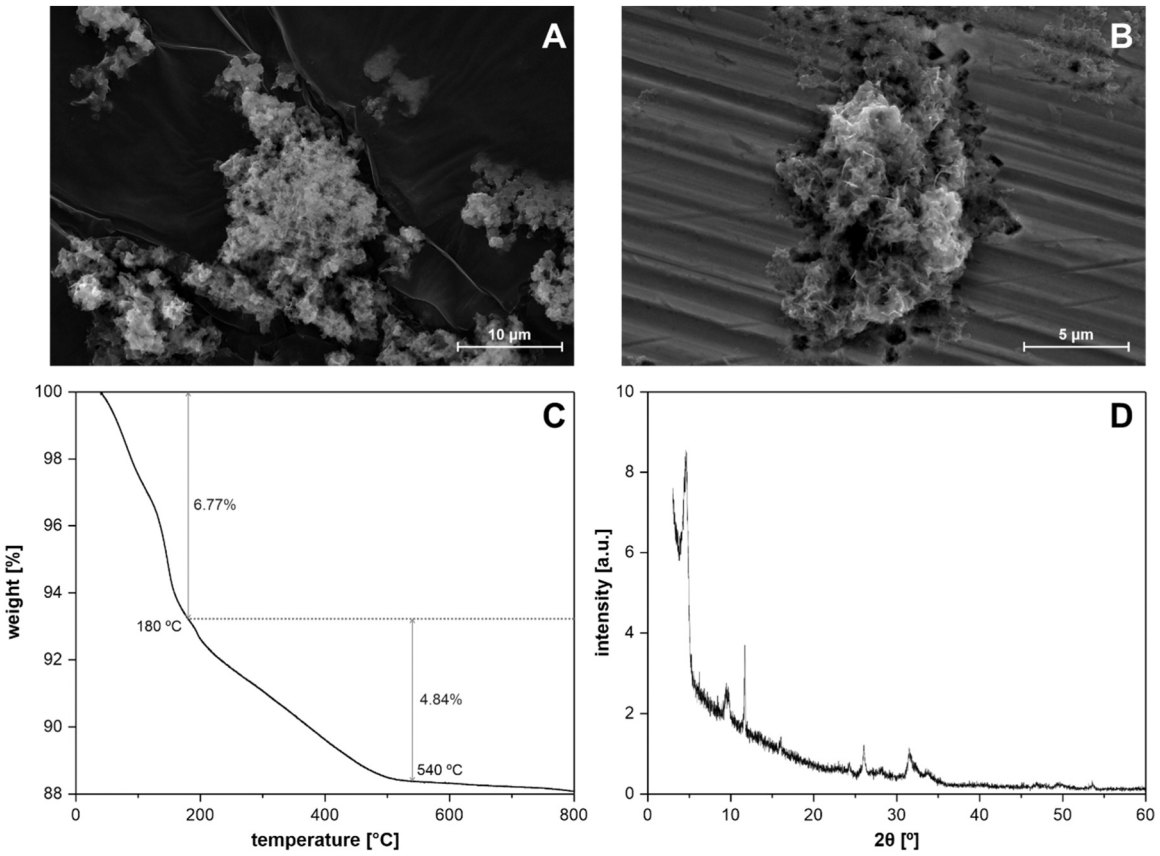

Fig. 3. A: SEM image of non-sputtered U-CaNFs drop casted on carbon adhesive registered in high vacuum mode; B: SEM image of carbon coated (ca. 5 nm) U-CaNFs drop casted on copper foil registered in high vacuum mode; C: Thermogravimetric analysis of U-CaNFs. D: XRD diffraction patterns measured for U-CaNFs.

and relatively short analysis time. In the beginning, various dilutions of nanoflowers, here defined as the volume of 100 mmol L^{-1} pH 7 Tris buffer used to suspend U-CaNFs after their assembly (see Section 2.3). The optimal pH for type III Jack bean urease is 7.4 [43], but we decided to use pH 7 buffer optimal for NH_4^+ detection, as in this case rising pH affects the measuring range significantly (as shown in Fig. S2B). For each of the tested U-CaNFs dilutions, the kinetic of colorimetric signal development was registered for 10 min in 1 min interval for 0 and 10 mmol L^{-1} urea. The results obtained are presented in Fig. S8. They clearly prove that the more diluted U-CaNFs are, the lower differences in signals are measured. This is an expected outcome as higher enzyme amount in a µTAD translates into more sites available for urea hydrolysis. Buffer volumes lower than 0.5 mL were not tested due to the fact that such solutions would be highly viscous, impeding reproductible immobilization on thread. Consequently, 0.5 mL Tris buffer was chosen as an optimal volume of U-CaNFs suspending solution.

U-CaNFs immobilized on thread were visualized using SEM and the pictures obtained are shown in Fig. 4A and B. The obtained pictures prove that U-CaNFs retain petal-like nanostructure after placing them on thread solid support. However, they are forming a film covering thread fibers, rather than maintaining individual nanoflower structure, as shown earlier in Fig. 3A and B. This is probably because the concentration of U-CaNFs is locally very high, causing nanoflowers aggregation. Additionally, an EDS map of the entire µTAD (prior to sensing cocktail introduction) was performed for phosphorus, carbon and calcium. This map is shown in Fig. 4D. U-CaNFs, represented by the presence of calcium and phosphorus, are localized in the center of the thread, exactly where they were introduced by the pipette. Strong carbon signal at thread ends stems from carbon-tape adhesive employed for SEM sample preparation. Clearly, U-CaNFs adhere to cellulose fibers and do not flow along with the buffer to uniformly cover the thread. This can either be caused by strong adhesion of U-CaNFs to thread fibers or be a result of micrometric size of nanoflowers, which can be 'filtered' by thread. The issue of U-CaNFs aggregation could be solved by diluting U-CaNFs, but as shown in Fig. S8, this compromises sensitivity of urea determination. Alternatively, thread surface could be modified with a chemical enabling U-CaNFs dispersion on thread. However, implementing such a modification would require detailed research to ensure U-CaNFs are evenly dispersed on thread, but NH_4^+ detection is not compromised.

Such localization of U-CaNFs on µTAD has direct implications on colorimetric signal. It causes uneven color change of the sensing membrane, which is shown in Fig. 4C. Pink color of the membrane is a result of high ammonium ions concentration and its location correlates with the location of U-CaNFs. Towards the beginning of the thread (here beginning is understood as the end of the thread where sample is introduced), the membrane is gradually more blue, indicating lower concentration of NH_4^+. Ammonium ions are formed only where U-CaNFs are immobilized and they do not diffuse to other parts of µTAD. Such poor uniformity of membrane color might lead to poor precision of the readings. Because of that, placement of U-CaNFs suspension in relation to the location of sensing membrane was optimized. Three setups were tested: membrane and U-CaNFs located in the center of the thread, U-CaNFs located in the beginning of the thread and membrane located in the center, and U-CaNFs located in the center while membrane was located in the end of the thread. In all of these setups, kinetics of colorimetric signal development were registered for 10 mmol L^{-1} urea and the uniformity of the resulting membrane color was compared. Based on the obtained kinetic data, shown in Fig. 4E, it can be established that U-CaNFs and membrane placement do not significantly influence colorimetric signal development. Although the highest hue intensity is measured for setup a (U-CaNFs in the beginning of the

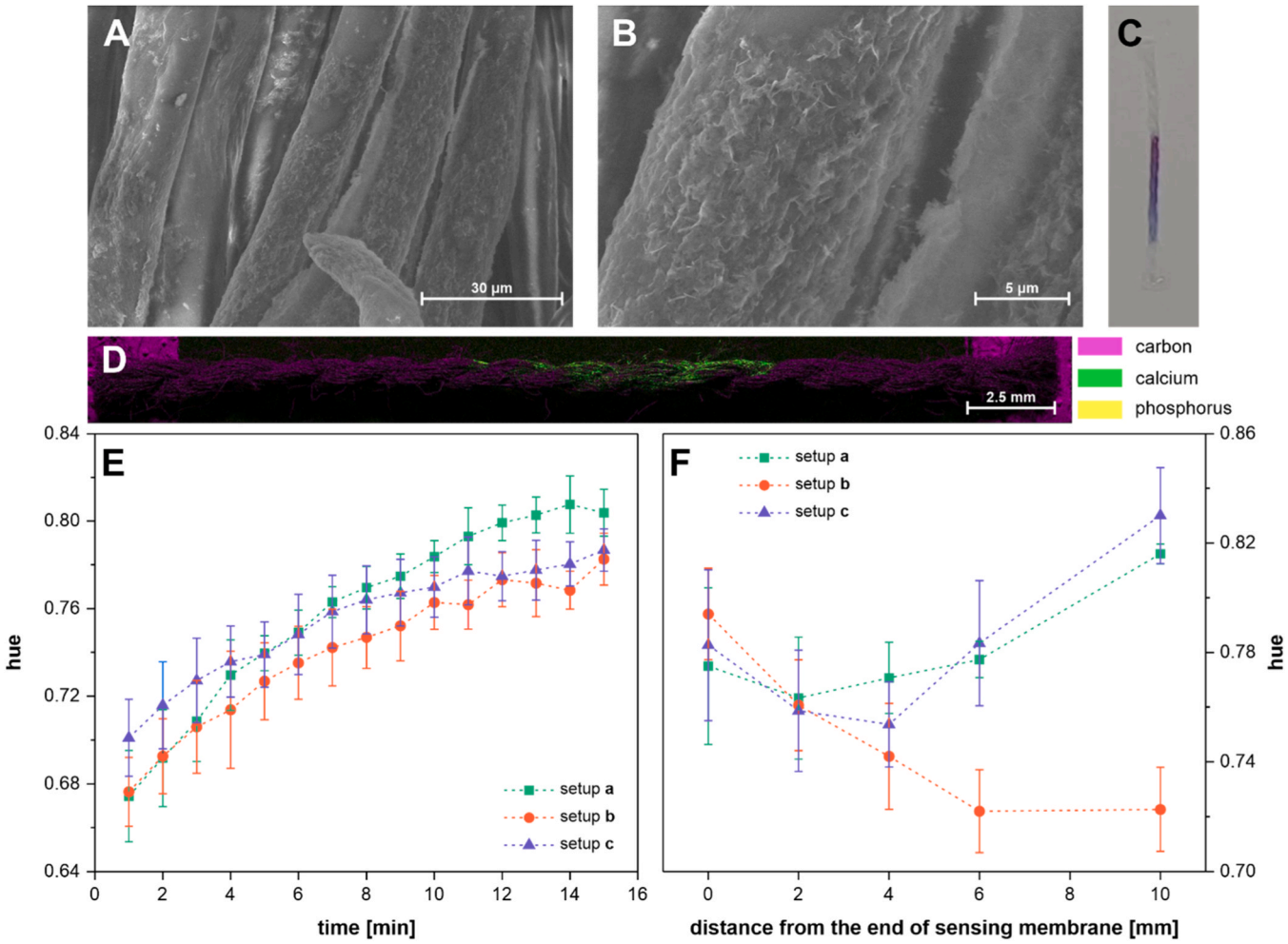

Fig. 4. A, B: Low vacuum SEM images of U-CaNFs immobilized on cotton thread; C: Photo of µTAD with U-CaNFs and sensing membrane immobilized in the middle of thread; D: Large area EDS mapping (of carbon, calcium and phosphorus) of the entire µTAD with immobilized U-CaNFs in the middle of the thread; E: Kinetics of colorimetric signal development for 10 mmol L^{-1} urea in the following setups: a – U-CaNFs immobilized in the beginning of the thread, sensing membrane immobilized in the middle of the thread, b – U-CaNFs and sensing membrane immobilized in the middle of the thread, c – U-CaNFs immobilized in the middle of the thread, sensing membrane immobilized in the end of the thread; F: Variation of colorimetric signal with the length of sensing membranes measured in the same setups as in E at 8 min of reaction time.

thread, membrane in the middle), the differences between all setups in measured hue intensity should not influence the assay performance in a clinically relevant way. On the other hand, the membrane color intensity profiles, presented in Fig. 4F, vary based on the placement of U-CaNFs and membrane. The lowest variations in hue intensity in a function of length of the membrane, indicating the highest color uniformity, are obtained when U-CaNFs are immobilized in the beginning of the thread and the sensing membrane located in the middle of the thread. As a consequence, in further experiments U-CaNFs are introduced in the beginning of the thread while sensing membrane cocktail is pipetted in the middle of the thread. Also, basing on data shown in Fig. 4E, the optimal reaction time was set to be 8 min as a compromise between high hue intensity and relatively short incubation time.

To undoubtfully prove, that urease immobilized in calcium phosphate nanoflowers is the agent responsible for urea hydrolysis, and also to establish the efficiency of this process in comparison to hydrolysis with free urease enzyme, calibration curves were registered in the following conditions: (i) µTAD sensitized with U-CaNFs with urea as analyte; (ii) µTAD sensitized with free urease (the same concentration as in U-CaNFs, i.e. 0.25 mg mL^{-1} in Tris buffer) with urea as analyte; (iii) µTAD buffered with Tris buffered with urea as analyte; (iv) µTAD sensitized with calcium phosphate (i.e. U-CaNFs without the enzyme) with urea as analyte; (v) µTAD sensitized with U-CaNFs with NH_4^+ ions as analyte. The results obtained are presented in Fig. 5. Based on these data, it is clear that urease in U-CaNFs is responsible for urea hydrolysis as using µTAD sensitized with calcium phosphate alone does not allow to register any measurable signal increase with increasing urea concentration. Secondly, using U-CaNFs as a method for urease immobilization allows to lower the detection limit in comparison to the use of free urease enzyme. This can be attributed to an increase in enzymatic activity when enzyme is immobilized as metal phosphate nanoflowers. Finally, the responses of µTAD sensitized with U-CaNFs towards urea and ammonium ions are similar, indicating complete transformation of urea into ammonium ions as a consequence of enzymatic reaction.

In the optimal conditions a calibration curve was registered in five replicates for each standard. The obtained calibration dependence is presented in Fig. 6. Boltzmann sigmoidal function was fitted to the data and the parameters of this fit are shown in the figure. Limit of detection was calculated basing on the signal for blank sample with 3.3 standard deviations of blank measurement. The calculated LOD was 37 µmol L^{-1} urea. Precision, expressed as relative standard deviation, was 1.27 % for 1 mmol L^{-1} urea. Long-term storage stability of the developed µTADs for urea determination was established in 4ºC and 20ºC with additional protection from light. To verify, if enzyme immobilized in U-CaNFs retains its ability to convert urea to NH_4^+ ions, for this experiment hue difference between 0.5 and 8 min reaction time was used as analytical

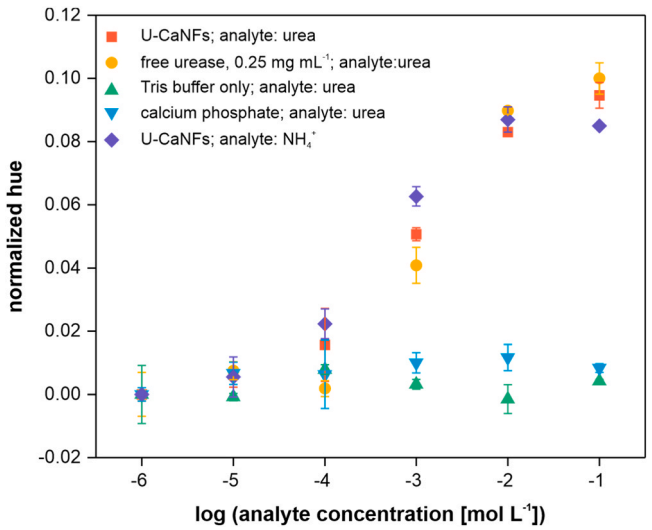

Fig. 5. Calibration dependencies registered using μTAD sensitized with U-CaNFs with urea as analyte, μTAD sensitized with free urease (the same concentration as in U-CaNFs, i.e. 0.25 mg mL^{-1} in Tris buffer) with urea as analyte, μTAD buffered with Tris buffered (without enzyme) with urea as analyte, μTAD sensitized with calcium phosphate (i.e. U-CaNFs without the enzyme) with urea as analyte, μTAD sensitized with U-CaNFs with NH_4^+ ions as analyte.

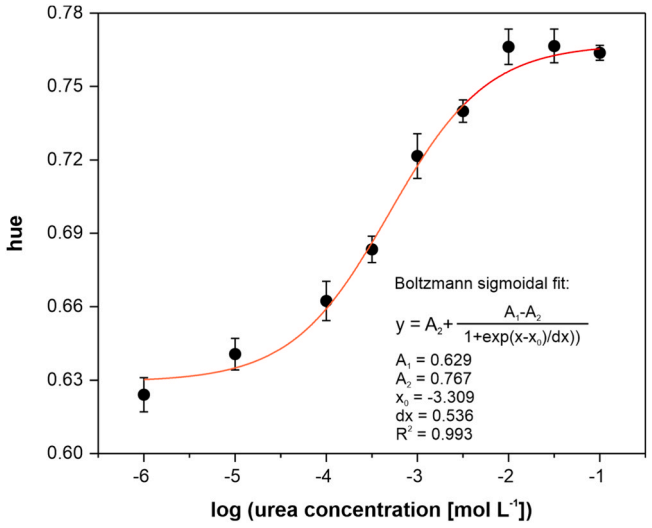

Fig. 6. Calibration curve for urea registered using the developed μTAD sensitized with U-CaNFs, n = 5.

signal. The results obtained, presented in Fig. S9, confirm that the stability of the developed μTAD in room temperature is very limited. This is probably an outcome of two processes: loss of enzymatic activity during storage and poor stability of the sensing membrane itself during storage [31,33]. On the other hand, μTADs stored at 4°C are reasonably stable for 2 weeks. Long-term stability of the sensing membrane could potentially be improved by switching Chromoionophore I to another lipophilic pH indicator with enhanced room temperature long-term stability. Another solution worth considering is impregnating hydrophilized cotton thread with chitosan. This should help both maintaining thread hydrophilicity for a long time [44] as well as stabilization of urease enzyme [45]. However, all of these potential fixes require targeted research and reoptimization of sensing conditions to ensure membrane response towards NH_4^+ remains sufficient for reliable urea determination.

The developed μTAD for urea determination was compared with other paper-based and thread-based disposable urea sensors published in the literature and the outcome is shown in Table 1. This comparison clearly shows that typically lowest limit of detection is achieved when NH_4^+ or NH_3 species ([19] and this work) are detected as products of enzymatic hydrolysis of urea rather than a change of pH. It is also important to highlight that the change of pH depends not only on urea concentration, but also on the buffer capacity of the sample, which might be problematic in case of complex biological samples such as serum, saliva or urine [7]. Additionally, among devices that employ smartphones for signal acquisition, the developed μTAD offers the lowest detection limit. This means that the proposed platform combines high analytical performance with the simplicity of smartphone-based detection which is advantageous over the paper- or thread-based devices found in the literature.

3.4. Real samples analysis

In the final stage of the project, urea was determined in six control sera samples to assess the developed μTAD accuracy. To cover a wide range of possible clinical scenarios, the used sera had physiological, too low or too high declared urea concentration. To accurately determine urea in serum samples, the influence of intrinsic ammonium ions (i.e. these not resulting from enzymatic urea hydrolysis) as well as ions interfering in NH_4^+ determination (Section 3.1) must be accounted for. To do that, serum samples were introduced both to μTAD for NH_4^+ detection (thread sensitized with Tris buffer and sensing membrane) and for urea detection (thread sensitized with U-CaNFs suspended in Tris buffer and sensing membrane). The analytical signal used in this case was a difference between hue intensity obtained with urea-μTAD and hue intensity obtained with NH_4^+-μTAD. A schematic representation of how analytical signal is calculated for real samples analysis is presented in Fig. S10 and the obtained results for urea determination in control sera are gathered in Table 2. All determined urea concentrations are within the range declared by serum manufacturers and the calculated relative errors confirm acceptable accuracy of the developed sensor. The declared urea concentration was measured using urease/glutamate dehydrogenase kinetic assay using clinical analyzers, which is a gold-standard urea determination method.

4. Conclusion

In this paper, we presented a thread-based microfluidic device for urea determination in serum samples. The detection scheme utilized enzymatic urea hydrolysis, followed by ammonium ions detection with ionophore-based optical sensor. Both processes occurred on a single piece of thread, making the detection process extremely user friendly. It is important to highlight, that that the developed device could be further modified with a whole blood separation membrane to broaden the spectrum of samples which could be analyzed [46]. Also, a smartphone application could be implemented to automatize signal acquisition and processing [32,47]. Finally, the same detection scheme can be implemented for creatinine determination provided urease is switched to creatinine deaminase. Combining urea and creatinine detection in a single thread-based analytical device is an exciting direction of further research as a comprehensive kidney function point-of-care test.

CRediT authorship contribution statement

Izabela Lewińska: Writing – review & editing, Writing – original draft, Validation, Methodology, Investigation, Funding acquisition, Data curation, Conceptualization. **Ignacio de Orbe-Payá:** Writing – review & editing, Writing – original draft, Validation, Data curation. **Paweł Bącal:** Writing – review & editing, Writing – original draft, Methodology, Investigation, Data curation. **Miguel M. Erenas:** Writing – review & editing, Writing – original draft, Visualization, Supervision, Funding acquisition, Conceptualization. **Luis Fermín Capitán-Vallvey:** Writing

Table 1
Comparison of the developed thread-based analytical device with other thread- or paper-based devices for urea determination published in the literature. BTB – bromothymol blue, nd – no data, NPs – nanoparticles, GO – graphene oxide.

detection method	solid support	samples	detector	limit of detection [mmol L^{-1}]	response time	reference
enzymatic colorimetric with phenol red	paper	saliva	smartphone	1.7	20 s	[17]
enzymatic colorimetric with BTB	paper	blood	custom-made optical reader	0.03	2 min	[15]
enzymatic colorimetric with BTB	paper	saliva	scanner	0.049	35 min	[14]
enzymatic colorimetric with phenol red	thread	artificial sweat	smartphone with macro lens	30	nd	[18]
enzymatic colorimetric with Prussian blue NPs	paper	milk, artificial urine	smartphone	0.27	15 min	[16]
enzymatic colorimetric using thiomalic acid-NPs and maltol NPs	paper	saliva, plasma	scanner	0.03	3 min	[19]
change of resistance when NH_4^+ reacts with polystyrene sufonate	paper	saliva	multimeter	1.6	60 s	[20]
direct electrochemical detection using electrode modified with NiS/GO	thread	saliva	potentiostat	0.007	nd	[21]
enzymatic colorimetric with NH_4^+-sensitive optodes	thread	serum	smartphone	0.037	8 min	this work

Table 2
Analysis of urea content in control sera samples. *relative error was calculated in relation to declared average urea concentration.

Sample name	Declared urea concentration range [mmol L^{-1}]	Declared average urea concentration [mmol L^{-1}]	Dilution factor	Determined urea concentration [mmol L^{-1}]	Relative error*
Cormay Human Normal	4.80 – 6.10	5.45	25	5.27	-3.3 %
Cormay Human Pathological	14.5 – 18.5	16.5	25	14.1	-14.5 %
BioMaxima BioNorm	5.47 – 7.39	6.43	25	7.02	9.2 %
BioMaxima BioPath	16.2 – 21.9	19.1	25	16.1	-15.7 %
Pointe Scientific N	1.82 – 2.49	2.16	15	1.99	-7.9 %
Pointe Scientific P	7.78 – 9.10	8.44	25	9.83	16.4 %

– review & editing, Writing – original draft, Supervision, Funding acquisition, Conceptualization.

Declaration of Competing Interest

The authors declare that they have no known competing financial interests or personal relationships that could have appeared to influence the work reported in this paper.

Acknowledgements

IL was supported by the Foundation for Polish Science (FNP). This research was funded by Spanish MCIN/AEI/10.13039/501100011033/ with project PID2022–138727OB-I00. The project was partially supported by European Regional Development Funds “ERDF A way of making Europe”. Junta de Andalucía project DGP_PIDI_2024_01237. Funding for open access charge: Universidad de Granada / CBUA.

Appendix A. Supporting information

Supplementary data associated with this article can be found in the online version at doi:10.1016/j.snb.2026.139644.

Data availability

Data will be made available on request.

References

[1] A.O. Hosten, Clinical Methods: The History, Physical, and Laboratory Examinations, 563–563, Ann. Intern. Med. 113 (1990), https://doi.org/10.7326/0003-4819-113-7-563_2.
[2] H. Wang, J. Ran, T. Jiang, Urea, in: B. Yang, J.M. Sands (Eds.), Urea Transporters, Springer, Dordrecht, 2014, pp. 7–29.
[3] I. Gutmann, H.U. Bergmeyer, Urea, in: H.U. Bergmeyer (Ed.), Methods of Enzymatic Analysis, Second Edition, Academic Press, 1979, pp. 1791–1801, https://doi.org/10.1016/B978-0-12-091304-6.50030-6.
[4] L. Quadrini, S. Laschi, C. Ciccone, F. Catelani, I. Palchetti, Electrochemical methods for the determination of urea: Current trends and future perspective, TrAC Trends Anal. Chem. 168 (2023) 117345, https://doi.org/10.1016/j.trac.2023.117345.
[5] P.S. Francis, S.W. Lewis, K.F. Lim, Analytical methodology for the determination of urea: Current practice and future trends, TrAC Trends Anal. Chem. 21 (2002) 389–400, https://doi.org/10.1016/S0165-9936(02)00507-1.
[6] A.J. Taylor, P. Vadgama, Analytical reviews in clinical biochemistry: The estimation of urea, Ann. Clin. Biochem 29 (1992) 245–264, https://doi.org/10.1177/000456329202900301.
[7] R. Koncki, Analytical aspects of hemodialysis, TrAC Trends Anal. Chem. 27 (2008) 304–314.
[8] M. Singh, N. Verma, A.K. Garg, N. Redhu, Urea biosensors, Sens. Actuators B Chem. 134 (2008) 345–351, https://doi.org/10.1016/j.snb.2008.04.025.
[9] C.S. Pundir, S. Jakhar, V. Narwal, Determination of urea with special emphasis on biosensors: A review, Biosens. Bioelectron. 123 (2019) 36–50, https://doi.org/10.1016/j.bios.2018.09.067.
[10] E. Noviana, T. Ozer, C.S. Carrell, J.S. Link, C. McMahon, I. Jang, C.S. Henry, Microfluidic Paper-Based Analytical Devices: From Design to Applications, Chem. Rev. 121 (2021) 11835–11885, https://doi.org/10.1021/acs.chemrev.0c01335.
[11] C. Zhang, Y. Su, Y. Liang, W. Lai, Microfluidic cloth-based analytical devices: Emerging technologies and applications, Biosens. Bioelectron. 168 (2020) 112391, https://doi.org/10.1016/j.bios.2020.112391.
[12] X. Weng, Y. Kang, Q. Guo, B. Peng, H. Jiang, Recent advances in thread-based microfluidics for diagnostic applications, Biosens. Bioelectron. 132 (2019) 171–185, https://doi.org/10.1016/j.bios.2019.03.009.
[13] L.P. Murray, C.R. Mace, Usability as a guiding principle for the design of paper-based, point-of-care devices – A review, Anal. Chim. Acta 1140 (2020) 236–249, https://doi.org/10.1016/j.aca.2020.09.063.
[14] F.T.S.M. Ferreira, R.B.R. Mesquita, A.O.S.S. Rangel, On-hand tool for ammonium and urea determination in saliva to monitor chronic kidney disease – Design of a couple of microfluidic paper-based devices, Microchem. J. 193 (2023) 0–7, https://doi.org/10.1016/j.microc.2023.109102.
[15] J. Cheng, Y. Fu, J. Guo, J. Guo, A low-cost paper-based blood urea nitrogen optical biosensor for renal surveillance in fingertip blood, Sens. Actuators B Chem. 387 (2023) 133795, https://doi.org/10.1016/j.snb.2023.133795.
[16] W.Y. Zhang, C.Y. Zhang, H.Y. Zhou, T. Tian, H. Chen, H. Zhang, F.Q. Yang, Paper-based sensor depending on the Prussian blue pH sensitivity: Smartphone-assisted detection of urea, Microchem. J. 181 (2022) 107783, https://doi.org/10.1016/j.microc.2022.107783.
[17] A. Soni, R.K. Surana, S.K. Jha, Smartphone based optical biosensor for the detection of urea in saliva, Sens. Actuators B Chem. 269 (2018) 346–353, https://doi.org/10.1016/j.snb.2018.04.108.

[18] N. Promphet, J.P. Hinestroza, P. Rattanawaleedirojn, N. Soatthiyanon, K. Siralertmukul, P. Potiyaraj, N. Rodthongkum, Cotton thread-based wearable sensor for non-invasive simultaneous diagnosis of diabetes and kidney failure, Sens. Actuators B Chem. 321 (2020) 128549, https://doi.org/10.1016/j.snb.2020.128549.
[19] A. Sheini, A paper-based device for the colorimetric determination of ammonia and carbon dioxide using thiomalic acid and maltol functionalized silver nanoparticles: application to the enzymatic determination of urea in saliva and blood, Microchim. Acta 187 (2020) 565, https://doi.org/10.1007/s00604-020-04553-8.
[20] R.J. Rath, J. Giaretta, T.P. Hoang, R. Zulli, S. Farajikhah, S. Talebian, S. Naficy, F. Dehghani, Cascading chemiresistive paper-based enzymatic biosensor for urea detection, Sens. Actuators Rep. 9 (2025) 100330, https://doi.org/10.1016/j.snr.2025.100330.
[21] Z. Zhao, J. Xiao, X. Zhang, J. Jiang, M. Zhang, Y. Li, T. Li, J. Wang, A thread-based micro device for continuous electrochemical detection of saliva urea, Microchem. J. 190 (2023) 108634, https://doi.org/10.1016/j.microc.2023.108634.
[22] Y.A. Yang, C.H. Lin, Y.C. Wei, Thread-based microfluidic system for detection of rapid blood urea nitrogen in whole blood, Microfluid. Nanofluidics 16 (2014) 887–894, https://doi.org/10.1007/s10404-014-1338-6.
[23] Y.A. Yang, C.H. Lin, Multiple enzyme-doped thread-based microfluidic system for blood urea nitrogen and glucose detection in human whole blood, Biomicrofluidics 9 (2015) 1–13, https://doi.org/10.1063/1.4915616.
[24] K.J. Land, D.I. Boeras, X.S. Chen, A.R. Ramsay, R.W. Peeling, REASSURED diagnostics to inform disease control strategies, strengthen health systems and improve patient outcomes, Nat. Microbiol 4 (2019) 46–54, https://doi.org/10.1038/s41564-018-0295-3.
[25] F. Fu, X. Zhang, W. Wang, X. Xie, Colorimetric Optode Sensor with Tripodal Ionophore for Rapid Urinary Ammonium Determination, ACS Sens. 10 (2025) 3757–3762, https://doi.org/10.1021/acssensors.5c00756.
[26] R. Koncki, G.J. Mohr, O.S. Wolfbeis, Enzyme biosensor for urea based on a novel pH bulk optode membrane, Biosens. Bioelectron. 10 (1995) 653–659, https://doi.org/10.1016/0956-5663(95)96955-X.
[27] B. Kovács, G. Nagy, R. Dombi, K. Tóth, Optical biosensor for urea with improved response time, Biosens. Bioelectron. 18 (2002) 111–118, https://doi.org/10.1016/S0956-5663(02)00164-1.
[28] C. Stamm, K. Seiler, W. Simon, Enzymatic biosensor for urea based on an ammonium ion-selective bulk optode membrane, Anal. Chim. Acta 282 (1993) 229–237, https://doi.org/10.1016/0003-2670(93)80206-Z.
[29] H. Chen, E. Wang, Optical urea biosensor based on ammonium ion selective membrane, Anal. Lett. 33 (2000) 997–1011, https://doi.org/10.1080/00032710008543104.
[30] L. Wang, J. Liao, D. Yuan, X. Xie, Colorimetric water hardness sensor optode containing neutral ionophore and chromoionophore, Sens. Actuators B Chem. 440 (2025) 137922, https://doi.org/10.1016/j.snb.2025.137922.
[31] M.M. Erenas, I. De Orbe-Payá, L.F. Capitan-Vallvey, Surface Modified Thread-Based Microfluidic Analytical Device for Selective Potassium Analysis, Anal. Chem. 88 (2016) 5331–5337, https://doi.org/10.1021/acs.analchem.6b00633.
[32] M.J. Arroyo, M.M. Erenas, I. de Orbe-Payá, K. Cantrell, J.A. Dobado, P. Ballester, P. Blondeau, A. Salinas-Castillo, L.F. Capitán-Vallvey, Thread based microfluidic platform for urinary creatinine analysis, Sens. Actuators B Chem. 305 (2020) 127407, https://doi.org/10.1016/j.snb.2019.127407.
[33] I. Lewińska, L.F. Capitán-Vallvey, M.M. Erenas, Thread-based microfluidic sensor for lithium monitoring in saliva, Talanta 253 (2023) 4–11, https://doi.org/10.1016/j.talanta.2022.124094.
[34] Y. Wan, Z. Xie, M. Cao, C. Zhang, Z. Feng, B. Tian, Z. Liu, Detection of urea in milk by urease-inorganic hybrid nanoflowers combined with portable colorimetric microliter tube, Microchim. Acta 191 (2024) 1–14, https://doi.org/10.1007/s00604-024-06734-1.
[35] H. Li, X. Yan, D. Kong, D. Su, F. Liu, P. Sun, X. Liu, C. Wang, X. Jia, G. Lu, Self-assembled multiprotein nanostructures with enhanced stability and signal amplification capability for sensitive fluorogenic immunoassays, Biosens. Bioelectron. 206 (2022) 114132, https://doi.org/10.1016/j.bios.2022.114132.
[36] K. Cantrell, M.M. Erenas, I. De Orbe-Payá, L.F. Capitán-Vallvey, Use of the hue parameter of the hue, saturation, value color space as a quantitative analytical parameter for bitonal optical sensors, Anal. Chem. 82 (2010) 531–542, https://doi.org/10.1021/ac901753c.
[37] E. Bakker, P. Bühlmann, E. Pretsch, Carrier-based ion-selective electrodes and bulk optodes. 1. General characteristics, Chem. Rev. 97 (1997) 3083–3132, https://doi.org/10.1021/cr940394a.
[38] M. Cuartero, N. Colozza, B.M. Fernández-Pérez, G.A. Crespo, Why ammonium detection is particularly challenging but insightful with ionophore-based potentiometric sensors-an overview of the progress in the last 20 years, Analyst 145 (2020) 3188–3210, https://doi.org/10.1039/d0an00327a.
[39] M.M. Erenas, I. Ortiz-Gómez, I. De Orbe-Payá, D. Hernández-Alonso, P. Ballester, P. Blondeau, F.J. Andrade, A. Salinas-Castillo, L.F. Capitán-Vallvey, Ionophore-based optical sensor for urine creatinine determination, ACS Sens. 4 (2019) 421–426, https://doi.org/10.1021/acssensors.8b01378.
[40] C. Altinkaynak, S. Tavlasoglu, N. Özdemir, I. Ocsoy, A new generation approach in enzyme immobilization: Organic-inorganic hybrid nanoflowers with enhanced catalytic activity and stability, Enzym. Microb. Technol. 93–94 (2016) 105–112, https://doi.org/10.1016/j.enzmictec.2016.06.011.
[41] B. Somturk, I. Yilmaz, C. Altinkaynak, A. Karatepe, N. Özdemir, I. Ocsoy, Synthesis of urease hybrid nanoflowers and their enhanced catalytic properties, Enzym. Microb. Technol. 86 (2016) 134–142, https://doi.org/10.1016/j.enzmictec.2015.09.005.
[42] B. Krajewska, Mono- (Ag, Hg) and di- (Cu, Hg) valent metal ions effects on the activity of jack bean urease. Probing the modes of metal binding to the enzyme, J. Enzym. Inhib. Med. Chem. 23 (2008) 535–542, https://doi.org/10.1080/14756360701743051.
[43] Urease Type III product information, ⟨https://www.sigmaaldrich.com/deepweb/assets/sigmaaldrich/product/documents/281/021/u1500enz.pdf⟩, accessed 16.10.2025.
[44] Y. Dan, L. Wan, Y. Li, H. Hui, C. Can, F. Yue, J. Kang, Chitosan functionalization to prolong stable hydrophilicity of cotton thread for thread-based analytical device application, Cellulose 25 (2018) 4831–4840, https://doi.org/10.1007/s10570-018-1891-3.
[45] S. Kumar, A. Dwevedi, A.M. Kayastha, Immobilization of soybean (Glycine max) urease on alginate and chitosan beads showing improved stability: Analytical applications, J. Mol. Catal. B Enzym 58 (2009) 138–145, https://doi.org/10.1016/j.molcatb.2008.12.006.
[46] M.M. Erenas, B. Carrillo-Aguilera, K. Cantrell, S. Gonzalez-Chocano, I.M. Perez de Vargas-Sansalvador, I. de Orbe-Payá, L.F. Capitan-Vallvey, Real time monitoring of glucose in whole blood by smartphone, Biosens. Bioelectron. 136 (2019) 47–52, https://doi.org/10.1016/j.bios.2019.04.024.
[47] I. Lewińska, M. Speichert, M. Granica, Ł. Tymecki, Colorimetric point-of-care paper-based sensors for urinary creatinine with smartphone readout, Sens. Actuators B Chem. 340 (2021) 129915, https://doi.org/10.1016/j.snb.2021.129915.

Izabela Lewińska received her PhD degree from University of Warsaw, Faculty of Chemistry in 2025. Her research is devoted to point-of-care creatinine sensing using paper-based analytical devices.

Pawel Bącal defended his PhD thesis in 2017 at University of Warsaw, Faculty of Chemistry. His research interest are material science with special focus on their micro-structural properties. Currently, he is an electron microscopy core facility manager at Institute of Paleobiology, Polish Academy of Sciences.

Ignacio de Orbe-Payá is Associate Professor of the Department of Analytical Chemistry at the University of Granada (Spain). He is currently working as a Researcher at the ECsens group, Department of Analytical Chemistry, University of Granada. His main areas of research are the development of the sensing phases for their use as chemical sensors in the determination of inorganic ions in several matrices; multivariate calibration methods for the quality control of pharmaceutical products and development of analytical methodology using solid-phase spectrometry

Luis F. Capitán-Vallvey, received his BSc in Chemistry (1973) and PhD in Chemistry (1986) from the Faculty of Sciences, University of Granada (Spain). In 1983, he founded the Solid Phase Spectrometry group (GSB) and in 2000, together with Prof. Palma López, the interdisciplinary group ECsens, which includes Chemists, Physicists and Electrical and Computer Engineers at the University of Granada. His current research interests are the design, development and fabrication of sensors and portable instrumentation for environmental, health and food analysis and monitoring. Recently is interested in printing chemical sensor and capillary-based microfluidic devices.

Miguel M. Erenas received the MSc degree (2004) and the PhD degree in Analytical Chemistry (2011) from the University of Granada (Granada, Spain). He is Associate Professor at the Department of Analytical Chemistry, University of Granada. His research interests include the use of imaging along with microfluidic disposable sensors based on thread and paper for bioanalysis and food quality analysis.